Journal of Hydrology: Regional Studies 48 (2023) 101466

Contents lists available at ScienceDirect

Journal of Hydrology: Regional Studies

journal homepage: www.elsevier.com/locate/ejrh

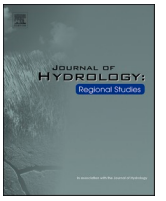

Managing coastal aquifer salinity under sea level rise using rice cultivation recharge for sustainable land cover

Ismail Abd-Elaty [a,*], Gehan A.H. Sallam [b], Lorenzo Pugliese [c], Abdelazim M. Negm [a], Salvatore Straface [d,e], Andrea Scozzari [f], Ashraf Ahmed [g,*]

[a] Department of Water and Water Structures Engineering, Faculty of Engineering, Zagazig University, Zagazig 44519, Egypt
[b] Drainage Research Institute (DRI), National Water Research Center (NWRC), Cairo, Egypt
[c] Department of Agroecology, Aarhus University, Blichers Allé 20, Tjele 8830, Denmark
[d] Department of Environmental and Chemical Engineering, University of Calabria, Ponte P. Bucci, 87036 Rende, Italy
[e] ISTI-CNR (Pisa), Italy
[f] CNR Institute of Information Science and Technologies (CNR-ISTI), Via Moruzzi 1, 56024 Pisa, Italy
[g] Department of Civil and Environmental Engineering, Brunel University London, Kingston Lane, Uxbridge, Sussex UB83PH, UK

ARTICLE INFO

Keywords:
Rice cultivation
Sea level rise
Seawater intrusion control
Saltwater intrusion
Incidental recharge
Nile Delta Aquifer

ABSTRACT

Study region: The coastal aquifer of Nile Delta, Egypt is used to develop the current study.
Study focus: Excess water from rice irrigation is a source of incidental recharge to mitigate seawater intrusion. This paper numerically explores the optimal location of rice cultivations by subdividing the delta domain into three distinct recharging regions (north, central and south). Additionally, SEAWAT code was simulated under a combination of rice cultivation relocation and sea level rise (SLR).
New hydrological insights for the region: The study findings revealed significant variations in salt volume reduction depending on the location of rice cultivation in the delta. Placing rice cultivation in the northern region resulted in the highest reduction of salt volume (19 %). In contrast, locating the recharge in the central region yielded a salt volume reduction of 0.50 %, while rice cultivation in the southern region produced a 15 % increase. Considering the projected SLR of 61 cm by 2100, there was an overall salt volume increment of 3 %. However, when accounting for both SLR and rice cultivation recharge in the northern region, a substantial salt volume reduction of 17 % was observed. The results demonstrated that incidental recharge by rice cultivation in coastal aquifers is an effective method for enhancing saltwater intrusion control. Moreover, this study improves our understanding of hydrological processes and expected responses in the delta under future climate scenarios.

Index of Abbreviations: 3D, 3 Dimensions; GWH, Groundwater Heads; MODFLOW, United States Geological Survey modular finite-difference flow model; MT3DMS, Modular Transport Three-Dimensional Multi-Species; MSL, Mean Sea Level; NDA, Nile Delta Aquifer; SWI, Saltwater intrusion; SLR, Sea Level Rise; SEAWAT, Three-Dimensional Variable-Density Groundwater Flow; TDS, Total Dissolved Concentration; USA, United States of America.

* Corresponding authors.
E-mail addresses: Eng_Abdelaty2006@yahoo.com (I. Abd-Elaty), Gehanhakeem@hotmail.com (G.A.H. Sallam), lorenzo.pugliese@agro.au.dk (L. Pugliese), amnegm85@yahoo.com (A.M. Negm), salvatore.straface@unical.it (S. Straface), Andscozzari@gmail.com (A. Scozzari), Ashraf.ahmed@brunel.ac.uk (A. Ahmed).

https://doi.org/10.1016/j.ejrh.2023.101466
Received 29 April 2023; Received in revised form 20 June 2023; Accepted 5 July 2023
Available online 17 July 2023

1. Introduction

Artificial recharge is a method utilized to recover groundwater resources by injecting water through wells from the ground surface (Bear et al., 1999; Abd-Elaty et al., 2021a). Near coastal areas in arid and semi-arid regions, irrigated agriculture has a great impact on the hydrological cycle and groundwater quality (Foster et al., 2018). In the presence of permeable soils, excess water naturally recharges freshwater into aquifers, reducing the intrusion of saltwater (Foster and Perry, 2009).

Saltwater intrusion (SWI) is a natural process occurring along coastal areas due to the higher density of the saline water compared to the fresh groundwater of the aquifer (Klassen and Allen, 2017; Abd-Elaty and Polemio, 2023). The extent of SWI depends on factors such as over pumping, seasonal variations in water recharge, tidal effects, barometric pressure, seismic waves, dispersion and Sea Level Rise (SLR) resulting from climate change (Bear et al., 1999; Dasgupta et al., 2018). According to the Intergovernmental Panel on Climate Change, the global mean SLR may vary between 26 and 82 cm by the year 2100 (IPCC, 2013). However, the rate of SLR is very variable on a geographical basis (Ketabchi et al., 2016; ESA SL-CCI, 2018).

Various techniques have been explored in recent decades to safeguard coastal aquifers from SWI, including relocation of fresh groundwater abstraction and recharge wells and installation of subsurface flow barriers (Abd-Elaty et al., 2022a; Luyun et al., 2011). More complex approaches involve the combination of abstraction, desalination and recharge or treatment, recharge, abstraction and desalination methods (Abd-Elhamid and Javadi, 2008; Abd-Elaty et al., 2021b). Abd-Elhamid and Javadi (2008) developed an Abstraction, Desalination and Recharge method consisting of three steps; the abstraction of brackish water from the saline zone, desalination of the abstracted brackish water using reverse osmosis treatment process, and recharge of the treated water into the aquifer. Roger et al. (2010) demonstrated that the subsurface flow barriers serve as physical barriers inserted across the flow direction to modify the flow field, rather than subsurface dams. Abd-Elaty et al. (2019a) used the SEAWAT code to evaluate the performance of physical subsurface barriers for controlling SWI in the Biscayne Aquifer in Florida, USA. They found that the cutoff wall gave higher retardation than subsurface dams. Abd-Elaty et al. (2020) employed different well systems by reducing pumping rates, recharge of treated wastewater, and abstraction of saline water to control SWI in coastal aquifers. Abd-Elaty and Zelenakova (2022b) compared the use of earth fills in shallow and deep coastal aquifers. The results showed that this method is more effective in managing SWI in shallow aquifers, rather than in deep ones.

The use of different types of physical barriers for layered heterogeneous aquifers was investigated by Abdoulhalik and Ahmed (2017a, 2017b). The existence of a low-permeability layer at the of bottom aquifer has slowed the effect of the barrier and slowed down the aquifer clean-up during the seawater retreat stage. Abdoulhalik et al. (2022) also examined the effective of cutoff walls to control seawater intrusion. Cutoff walls were found to be more effective in protecting freshwater wells against saltwater upconing when installed near pumping wells.

Extensive research has been conducted to simulate SWI and explore potential solutions for this problem using analytical and numerical models. Anwar (1983) investigated through analytical solutions the effect of a subsurface barrier into an unconfined coastal aquifer. Analytical solutions for controlling SWI in coastal aquifers through recharge fresh groundwater wells were presented by Hunt (1985). Tsanis and Song (2001) investigated numerically the installation of injection wells for reducing SWI. Recently, Abd-Elaty et al. (2022a) conducted numerical studies to demonstrate the reduction of SWI through abstraction and recharge processes in combination with coastal earth fill.

Although aquifer vulnerability and SWI have received growing attention worldwide due to their implications for water resource management, the majority of the modelling studies have considered remediation measures requiring high operation and maintenance costs (Roger et al., 2011; Hussain et al., 2019). From an economic perspective, the high costs associated with traditional remediation measures have posed challenges for resource-constrained regions, limiting their ability to address SWI effectively. In this context, the

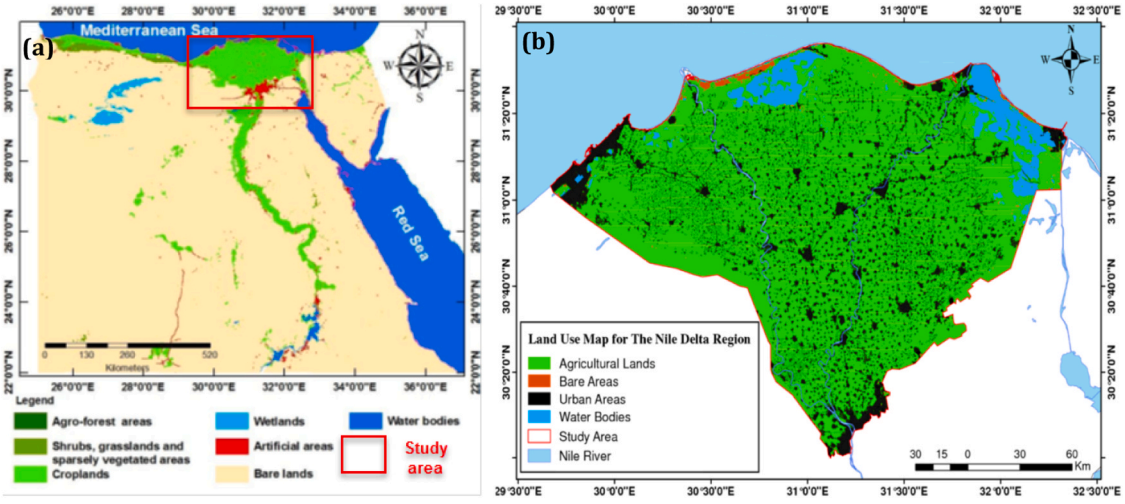

Fig. 1. Study area for (a) location map (Yossif, 2019) and (b) Land use/land cover (LULC) for the Nile Delta Aquifer (NDA) (El-Quilish et al., 2023).

use of modelling techniques and remedial strategies such as targeted incidental recharge can help identify economically viable solutions for coastal aquifer management. To the best knowledge of the authors, this study represents the first three-dimensional investigation modelling incidental recharge for SWI management in the Nile Delta Aquifer (NDA). The analysis encompasses three different scenarios, including the impact of the projected local SLR expected by the year 2100. The novelty of this work lies in its contribution to developing more sustainable management strategies for safeguarding coastal aquifers through the implementation of irrigated agriculture.

2. Material and methods

2.1. Study area

The NDA (30° 20`–31° 50`N; 30° 10`–31° 50`E), in Egypt, is delimited by the Damietta River in the south-east, the Rosetta River in the south-west and the Mediterranean Sea in the north (Fig. 1). Fluviomarine and Deltaic deposits are primarily found in the delta (Negm et al., 2018). Unconsolidated sand and gravel are generally identified, with sporadic and more interbedded clay lenses towards the north (MWRI, 2013; Abd-Elaty and Zelenakova, 2022b).

The aquifer is constituted by an upper clay cap and the underlying Quaternary aquifer. The average thickness of the semi-permeable clay layer varies from 50 m along the coast to 5–20 m in the south and central part (Diab et al., 1997). The average hydraulic conductivity of the clay cap is 2.5 mm day^{-1} in the vertical direction and varies between 50 and 500 mm day^{-1} in the horizontal direction (RIGW, 1992). The shallow Quaternary aquifer is constituted of Pliocene sticky clays and presents considerable variations in the lateral and vertical lithological faces. These variations lead to classify these deposits into a number of distinguishable horizons having specific hydrogeological characteristics (Nossair, 2011).

Recharge to the NDA comes from rainfall, river irrigation and canal seepage. The precipitation in the NDA varies from 25 mm year^{-1} in the south to 200 mm year^{-1} in the north (RIGW, 1992; Abd-Elaty et al., 2019b). The downward infiltration (net recharge) occurs by excess agriculture irrigation water (originating from the River Nile) and varies from 0.25 to 0.80 mm day^{-1}. Morsy (2009) presented a map for the aquifer showing a net recharge between 0.10 and 3.20 mm day^{-1}. Hamza et al. (1988) estimated an average total seepage from Ismailia Canal of 920 m^3 day^{-1}. The aquifer discharge occurs by seepage to waterways, inter-aquifer exchange flow, groundwater abstraction through wells and outflow to the sea (Molle et al., 2016). The average daily temperature and evaporation are 18.5 °C and 4 mm day^{-1} in the north and 25.0 °C and 7 mm day^{-1} in the south, respectively (SNC, 2010; WMRI-NWRC, 2002). Extraction wells in the NDA can be grouped into governmental irrigation production wells and drinking water production wells. The average yearly water produced by the well extraction in the entire region increased from 3.0 in 1992–5.0 billion cubic meters in 2008 (Morsy, 2009). The water table of the shallow aquifer varies in depth between 1.0 and 2.0 m in the north and between 3.0 m and 4.0 m in the central region, while it reaches almost 5.0 m in the south.

2.2. The numerical model

The latest version of SEAWAT, coupling MODFLOW and MT3DMS to integrate the density-dependent flow and the solute transport equation, was used. This integration ensures that changes in flow conditions are accurately represented in the transport simulations, leading to more realistic results. Additionally, MODFLOW and MT3DMS are highly versatile and widely used models, capable of simulating complex hydrogeological systems (Guo and Langevin Christian, 2002; Langevin and Guo, 2006), Machine learning algorithms or models for flow time series modelling were disregarded due to their limitations in comparison to MODFLOW, although some recent studies have shown promising results (Roy and Datta, 2017; Lin et al., 2019; Tao et al., 2021). These limitations include (i) the lack the physical interpretability and mechanistic representation of groundwater flow processes and (ii) the interpretation of the results.

The three-dimensional variable-density groundwater flow is described by the coupled system of flow and transport equations (Langevin et al., 2008):

$$\begin{aligned} \phi\frac{\partial\rho}{\partial t} - \nabla\left(\frac{\rho K}{\mu}(\nabla p + \rho g\nabla z)\right) = 0 \\ \phi\frac{\partial(\rho C)}{\partial t} + \nabla(\rho q C) - \phi\nabla(\rho D\nabla C) = 0 \end{aligned} \quad (1)$$

where ϕ is porosity; t is the time; K is the hydraulic conductivity tensor; p is pressure; μ and ρ are viscosity and fluid density, respectively; g is the gravitational constant; z is the space variable; C is the solute (salt) concentration; $D = (\phi d + \alpha_T|v|)I + (\alpha_L - \alpha_T)\, v\, v^T/|v|$ is the hydrodynamic dispersion tensor and d the diffusion coefficient; α_T and α_L are transverse and longitudinal dispersivity, respectively; $\boldsymbol{v} = q/\phi$ is the pore fluid velocity, and the superscript T denotes transpose. System (1) is closed by specifying a constitutive relationship, $\rho = \rho f + \beta C$, where $\beta = (\rho_s - \rho_f)/C_s$, ρ_s and ρ_f being salt and freshwater density respectively, and C_s the saltwater concentration.

2.2.1. Model geometry and boundary conditions

The model domain stretched for 150 km from the north (shoreline) to the south and 153 km from east to the west, covering an area of about 7800 km^2 (Fig. 2). A cell size of 1 × 1 km^2 was selected. A number of eleven layers having a total thickness ranging from

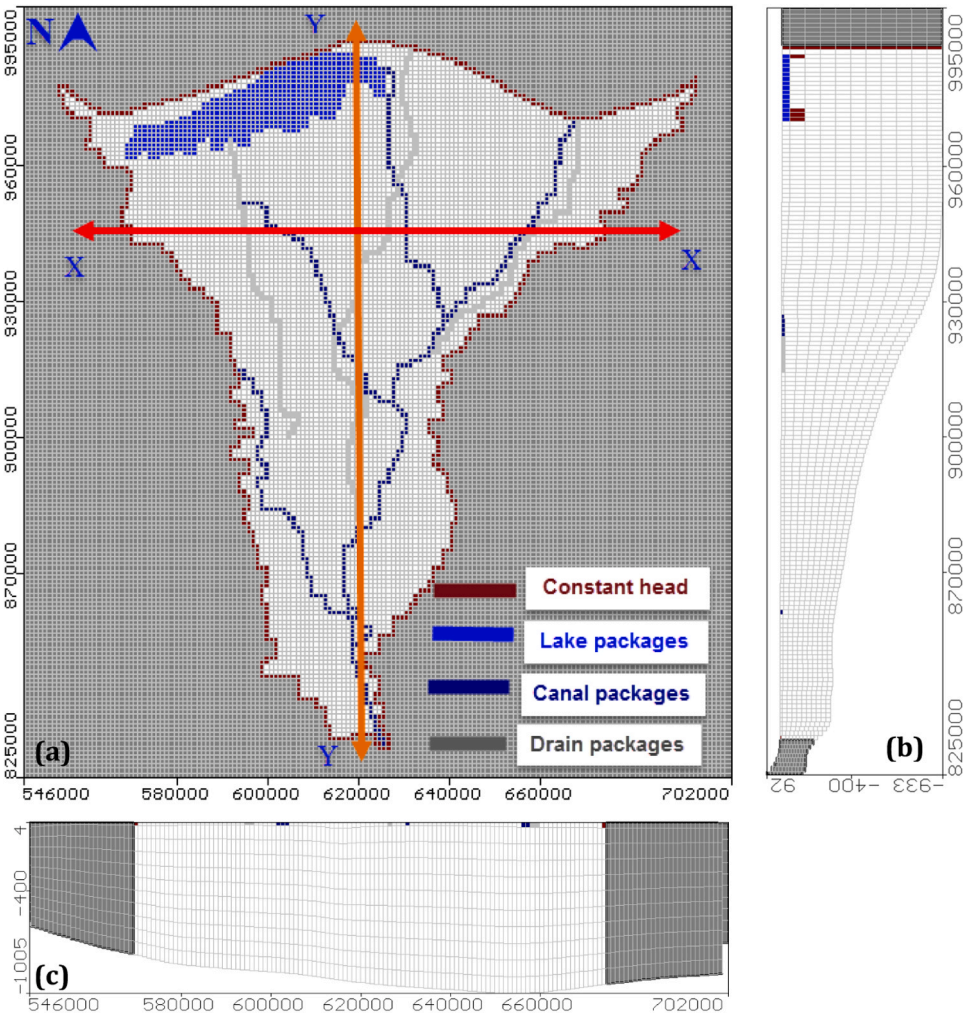

Fig. 2. Model geometry and boundary conditions for the Nile Delta Aquifer (NDA) according to the (a) aerial view and (b; c) vertical longitudinal cross-section views.

200 m near Cairo to 1000 m at the shoreline were implemented. The top layer represented the clay cap, with a depth ranging between 20 m in the south to 50 m in the north, while the remaining evenly-spaced layers represented the Quaternary aquifer.

A constant head equal to zero m was assigned at the north due to the fixed head of the Mediterranean Sea and 16.96 m was assigned to the south boundary due to the fixed head of the Nile River. Variable hydraulic heads were set to the west side of the aquifer (from 0.50 in the north to 13.17 m in the south) and to the east (from 0.50 in the north to 13.66 m in the south) due to the water levels in irrigation canals and streams. The initial Total Dissolved Concentration (TDS) for the NDA was set to zero mg/l, while a constant concentration of 40,000 and 35,000 mg/l were assigned at the north and to the Burullus Lake, respectively (Abd-Elhamid et al., 2016; Abd-Elaty and Zelenakova, 2022b).

2.2.2. Model hydraulic parameters

The horizontal hydraulic conductivity was set equal to 0.25 m day^{-1} and 100 m day^{-1} for the clay cap and the Quaternary aquifer layers, respectively. The vertical hydraulic conductivity varied between 0.0025 m day^{-1} and 10 m day^{-1} across the model domain. Additionally, the specific yield varied between 1×10^{-3} and 2×10^{-3}, while the effective porosity ranged from 20 % to 50 %. For the longitudinal dispersivity (α_L), transverse dispersivity (α_T) values are 100 m, 10 m and the diffusion coefficient (d) is 10^{-4} m^2 day^{-1} were assigned, respectively (Morsy, 2009; Abd-Elaty et al., 2019b). These values were used in the conceptual model as input components by using the river package interface, in addition to the river stage level, bottom level, river bed, vertical hydraulic conductivity, river bed thickness and conductance. The total average recharge, based on the hydrological balance, was set in the range between 0.15 and 1.10 mm day^{-1} depending on the soil type, evaporation, and irrigation and drainage practices (Fig. 3). The low values of recharge (0.15 mm day^{-1}) in the south are primarily due to the presence of water salinity. In contrast, the high values of recharge for the central and north regions (0.15 mm day^{-1} and 1.1 mm day^{-1}, respectively) mainly result from the absence of water

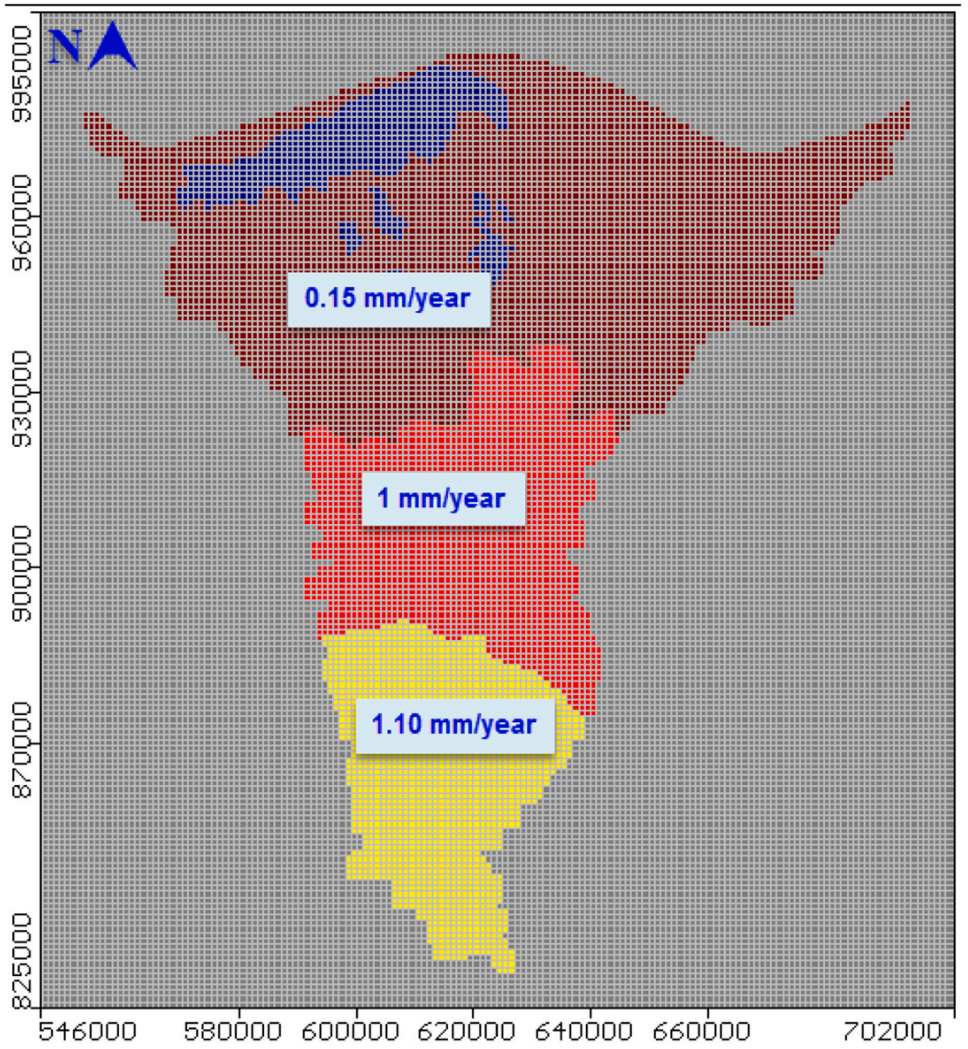

Fig. 3. Distribution map of recharge regions in the simulated Nile Delta Aquifer (NDA).

salinity. The abstraction from the NDA was set equal to 0.81 × 10^9 m^3 $year^{-1}$ (Morsy, 2009; Abd-Elaty et al., 2021c).

2.2.3. Model calibration and validation

The model calibration was performed using the groundwater heads (GWH) measurements from 18 observation wells located within the model domain (Fig. 4a). The initial time step was set to 0.01 days and the calibration period covered 500 years to reach a steady state and simulate the intrusion interface. The target error between the calculated and measured GWH was set equal to 10 % of the differences between the maximum and minimum values to reach 1.40 m. The model results indicated that the GWH in the NDA varied from 14 m above mean sea level (AMSL) at Cairo to 0 m (AMSL) at the shoreline (Fig. 4b). The minimum velocity occurring for the clay cap layer was 0.0019 m day^{-1} and the average velocity for the quaternary layers was 0.0668 m day^{-1}. The total inflow and outflow were 4,439,500 and 4,439,448 m^3 day^{-1}, respectively. These results were in agreement with those of Morsy (2009), thus proving the validity of the groundwater flow model.

The calibrated model water balance analysis is presented in Table 1 to show the contribution of total inflow and outflow. The total inflow was reached 976,830 m^3 day^{-1}, 3,610,100 m^3 day^{-1} and 77,590 m^3 day^{-1} with percentage of 20.94 %, 77.39 % and 1.66 % for constant heads, inflow to the aquifer and streams leakage respectively. The water budget analysis for outflow was reached 1,539,800 m^3 day^{-1}, 574,890 m^3 day^{-1}, 2,221,900 m^3 day^{-1} and 327,960 m^3 day^{-1} with percentage of 33.01 %, 12.32 %, 47.63 % and 7.03 % for constant heads, streams leakage, wells and drains respectively. The total inflow and the outflow reached 4,664,520 m^3 day^{-1} and 4,664,550 m^3 day^{-1} respectively.

The TDS results obtained from model calibration showed that Equi-line 1 (1000 ppm) by 103 km from the shoreline with a transition zone equal to 38 km and Equi-line 35 (35,000 ppm) moved inland by a distance of 65 km (Figs. 4c and 4d). These distances were estimated by taking into account the deepest point of each Equi-line, which, due to the density flow dependence coincides with

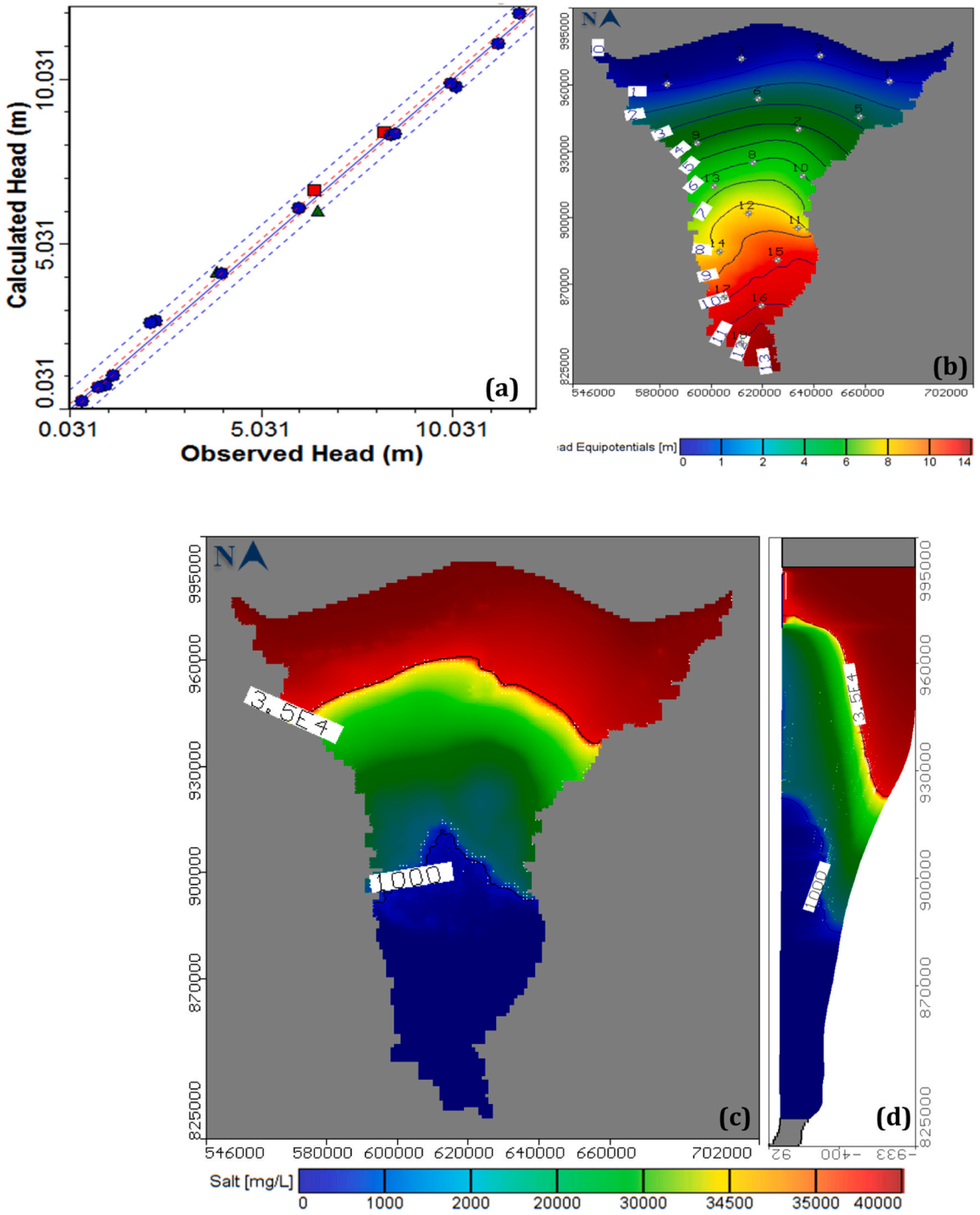

Fig. 4. Results from (a) calibration and (b) Groundwater Heads (GWH) by the SEAWAT transport model. The location of observation wells is also reported. Total Dissolved Solids (TDS) according to (c) aerial view and (d) vertical longitudinal cross section view.

the maximum intrusion point.

2.3. Projection of sea level rise

A possible SLR by 2100 was evaluated under the second scenario to investigate the impact on GWH and salinity. Initially, an average SLR value of 56 cm (AMSL) was considered, based on local estimates of SLR rate and acceleration derived from satellite radar altimetry (Legeais et al., 2018; Nerem et al., 2018; ESA SL-CCI, 2018). Data supplied by the ESA Sea-Level Climate Change Initiative

Table 1
Water balance parameters for the calibrated model.

Parameter	Input		Output		Input-Output
	$m^3\ day^{-1}$	%	$m^3\ day^{-1}$	%	$m^3\ day^{-1}$
Constant heads	976,830	20.94	1,539,800	33.01	-562,970
Flow into the aquifer	3,610,100	77.39	0	0	3,610,100
Canals leakage	77,590	1.66	574,890	12.32	-497,300
Wells	0	0	2,221,900	47.63	-2,221,900
Drains	0	0	327,960	7.03	-327,960
Total	**4,664,520**	**100**	**4,664,550**	**100**	**30**

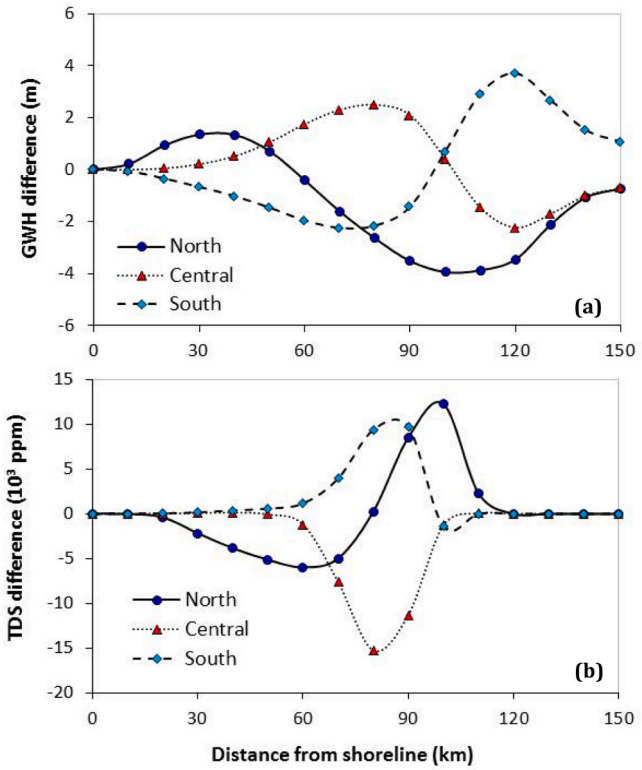

Fig. 5. A function of the distance from the shoreline for different recharge locations for (a) groundwater Head (GWH) (b) and Total Dissolved Solids (TDS) differences (b).

project included a gridded dataset with an SLR rate estimated by considering the year 2016 as a reference. This dataset permitted a more precise local estimate of future SLR increment in the region of interest. Selected grid points along the coast of the Nile Delta showed SLR rates spanning from 2.46 to 3.93 mm $year^{-1}$, implying a cumulated SLR at the time horizon of the year 2100 of about 49.20–61 cm (AMSL), respectively (Fig. A1, Appendix).

2.4. Scenario analysis

The NDA area was subdivided into three recharging regions (north, central and south), each one being 50–60 km wide. The calibrated model for the study area was simulated using three scenarios assigned to the north, central and south regions, respectively. Subsequently, the recharge for the first scenario was re-distributed by assigning each time 75 % of the total NDA recharge (base case) to one of the three regions.

3. Results and discussion

3.1. Impact of rice recharges location

The location of rice recharge in different regions resulted in distinct effects on groundwater hydrodynamics. When rice recharge

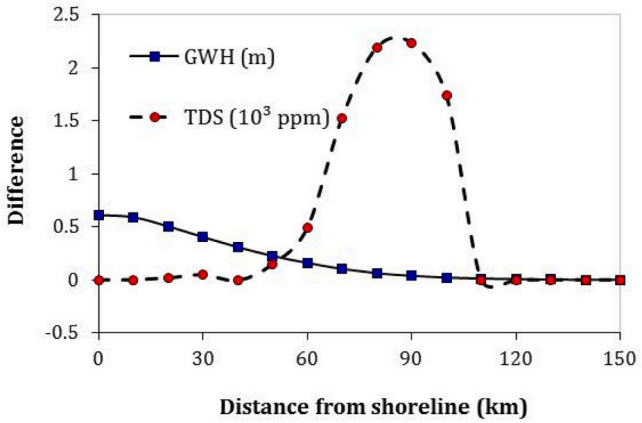

Fig. 6. Groundwater Head (GWH) and Total Dissolved Solids (TDS) differences as a function of distance from the shoreline for a Sea Level Rise (SLR) of 61 cm.

was concentrated in the northern region, there was an initial increase of the GWH within the first 55 km from the coastline, followed by a subsequent decrease towards the southern aquifer border (Fig. 5a). Recharging in the central region led to an increase in GWH between 30 and 100 km from the shoreline, followed by a decrease towards the southern aquifer border (Fig. 5a). Conversely, placing the recharge in the southern region caused a decrease in GWH from the shoreline until approximately 100 km inland, followed by an increase going further to the south (Fig. 5a).

The Equi-line 1, representing a specific groundwater contour, was reached at a distance of 111 km, 86 km and 94 km from the shoreline (Fig. A2, Appendix). The Equi-line 35 was reached at an average distance of 41 km, 61 km and 74 km from the shoreline for the corresponding regions. The extension of the transition zone (in green), indicating the presence of brackish water, was largest for recharge in the north, smaller and smallest in the central and south regions, with values of 70 km, 25 km and 20 km, respectively.

The largest variations of TDS concentration, due to the diverse rice recharge locations hypothesized in this paper, occurred in the central area of the NDA (Fig. 5b). Recharge in the north resulted in a reduction of TDS between 20 km and 80 km from the shoreline, followed by an increase from 80 km to 120 km. Rice recharge in the central region led to a decrease in TDS concentration between 50 km and 100 km from the shoreline, with significant variations observed elsewhere (Fig. 5b). Recharge in the south region showed an increase in TDS concentration between 40 km and 100 km from the shoreline, followed by a minor decrease (Fig. 5b).

Overall, the model results demonstrated that by locating the recharge in the northern region the SWI was mitigated substantially, with the SWI being the closest to the shoreline (Fig. A2a, Appendix). However, the distribution map of TDS for recharge in the north revealed a significant volume of fresh water in the recharging area. Conversely, when the recharge was located in the central (Fig. A2b, Appendix) and southern (Fig. A2c, Appendix) regions, a progressive inland advancement of the SWI front was observed. The salt mass balance reached 3.54028×10^{13} kg, 4.33963×10^{13} kg, and 5.04294×10^{13} kg for the northern, central, and southern regions, respectively, compared to 4.36916×10^{13} kg for the base case. The salt volume variation due to rice recharge location was + 19 %, + 0.50 % and − 15 % for the northern, central and southern regions, respectively. These findings align with earlier studies, investigating the impact of artificial recharge location on groundwater hydrodynamics and SWI. A study conducted by Motallebian et al. (2019) explored the effect of a recharge canal on the reduction rate in the extent of the saltwater intrusion. Their results showed that effective saltwater repulsion was achieved when the recharge canal was located near the toe of the saltwater wedge. This is also supported by earlier laboratory-scale experiments and numerical simulation (Luyun et al., 2011; Rasmussen et al., 2013). These comparative studies highlight the complex nature of groundwater dynamics and saltwater intrusion processes, which can be influenced by local geological, hydrological, and agricultural factors. The variations observed in different aquifer systems emphasize the importance of conducting site-specific investigations to tailor management approaches to the unique characteristics of each region.

3.2. *Impact of sea level rise*

The maximum increase of GWH due to SLR occurred near the shoreline and equalled to 61 cm (AMSL) (Fig. 6). Values of GWH gradually decreased towards the south and the effect of SLR became negligible at approximately 110 km inland.

Under the SLR scenario, the model results indicated that the SWI reached 106 km from the shoreline for Equi-line 1 and 67 km for Equi-line 35, with a transition zone width of approximately 39 km (Fig. A3, Appendix). The Nile Delta aquifer salt volume increased by 3 %. Thus, the SLR moved Equi-line 1 more than Equi-line 35, increasing the intrusion of saltwater and the width of the transition zone. The results for the TDS variations indicated that the SWI increased between 40 km and 110 km from the shoreline while no significant changes were observed within the range of 0–40 km, primarily due to the constant position of Equi-line 35 (Fig. 6).

The findings highlight the vulnerability of coastal aquifers to SLR-induced SWI. Changes in SLR can potentially move the seawater interface by hundreds of meters (Meyer et al., 2019; Costall et al., 2020; Jasechko et al., 2020). A 3D transient density-driven groundwater water demonstrated that an SLR of 0.5 m per century in a Dutch coastal aquifer would increase the salinity of all

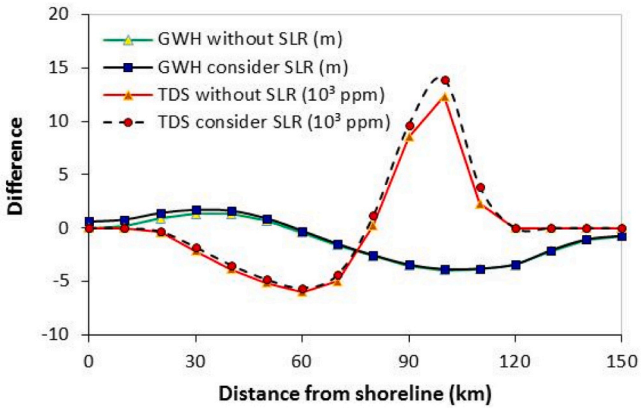

Fig. 7. Groundwater Head (GWH) and Total Dissolved Solids (TDS) differences as a function of distance from the shoreline for a Sea Level Rise (SLR) of 61 cm and recharge location in the north.

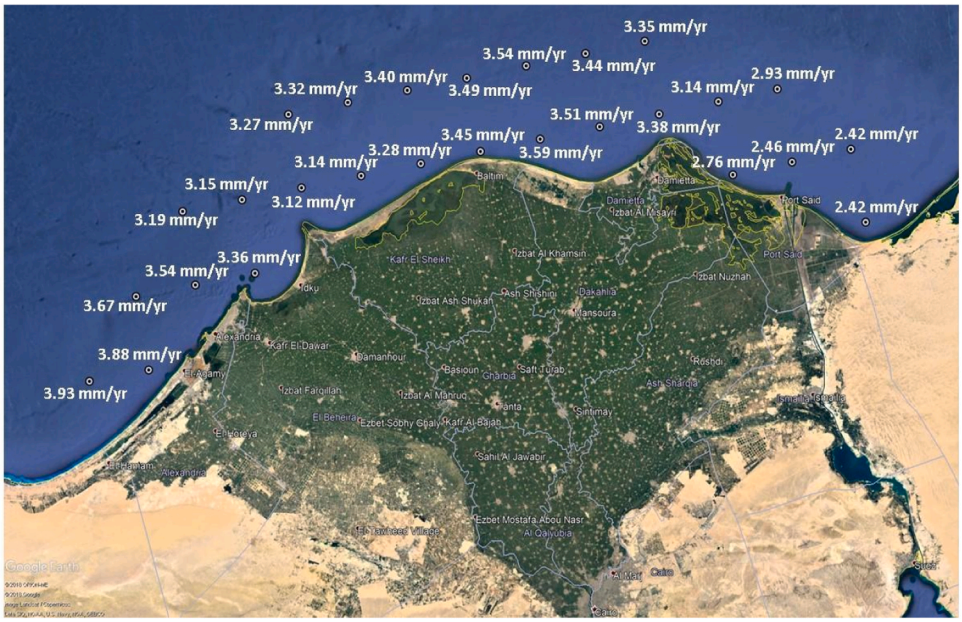

Fig. A1. Estimated Sea Level Rise (SLR) rates along the northern coast of the Nile delta (ESA SL-CCI data referred to year 2016 projected onto a Google Earth image).

low-lying regions closer to the sea (Oude Essink, 2001). The effect is amplified with the presence of karstic high-flow conduits (Xu et al., 2018). While the results presented so far appear reasonable, a recent review of the impact of SLR on coastal areas has highlighted certain limitations (Ketabchi et al., 2016). The majority of the conducted studies have focused only on a subset of known or anticipated controlling factors. Specifically, these studies have not addressed more realistic complexities, such as sloping aquifers, gradual SLR and uncertainties in defining model parameters, along with their implications for decision-making models (Shi et al., 2020). Consequently, additional research is necessary to comprehensively assess the effect of SLR and integrate these controlling factors into a holistic framework.

3.3. Impact of combined rice recharge location and sea level rise

The maximum increase of GWH due to SLR occurred near the shoreline, specifically in the northern region with an elevation difference of 61 cm (Fig. 7). Following the modelling results considering diverse rice recharge locations, the rice cultivation was assigned to the north of the NDA in combination with an SLR of 61 cm (AMSL). The GWH for this scenario initially increased and at 30 km from the shoreline gradually started decreasing (Fig. 7).

The SWI reached 111 km for Equi-line 1, with a transition zone that was 68 km wide, beginning 43 km from the shoreline for Equi-

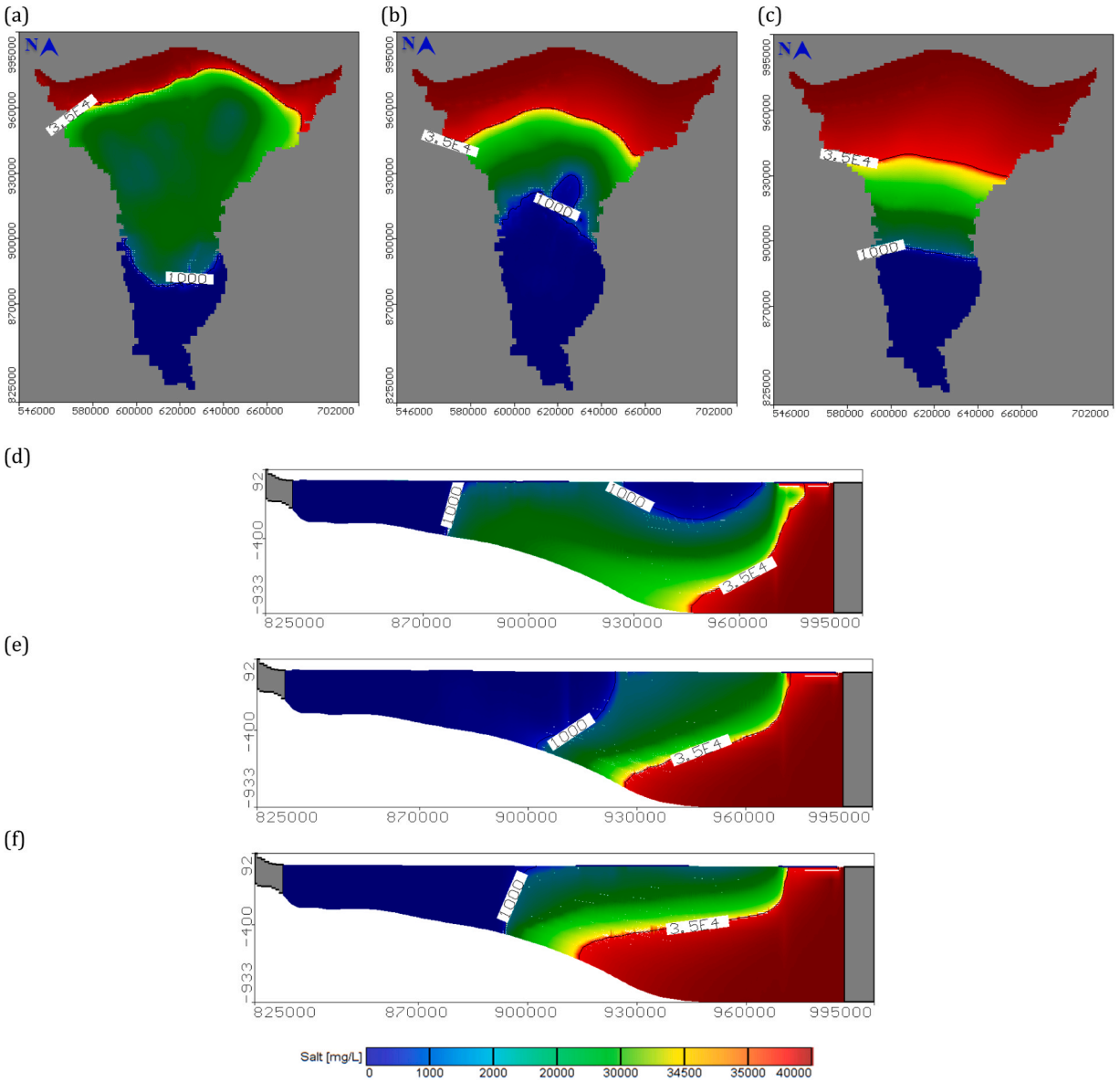

Fig. A2. Distribution of TDS for recharge in the north (left), center (middle) and south (right) of the Nile Delta Aquifer (NDA) according to vertical aerial (a–c) and longitudinal (d–f) view.

line 35 (Fig. 7, Fig. A4 in Appendix). The results indicated that the combination of rice cultivation in the north and SLR extended the transition zone, shifting Equi-line 1 approximately 8 km inland and Equi-line 35 about 31 km towards the coast, due to its average distance of 23 km from the coastline. The corresponding salt volume variation was equal to + 16.50 % compared with + 19 % for recharge only at the north, and − 3 % when considering SLR alone. Under this scenario, the salt mass balance reached 4.50325×10^{13}, compared to 3.63967×10^{13} kg obtained by only applying the recharge in the northern region. Results in terms of TDS indicated that under this scenario the aquifer's salinity would slightly decrease in the north for the Equi-line 35 until about 80 km from the shoreline, while it would slightly increase from 80 km to 120 km (Fig. 7).

The sustainable management of coastal aquifers is an ongoing and increasingly important environmental issue for many countries. In particular, the mitigation of SWI is a major problem for the territories that rely on groundwater resources in the coastal zone. The sustainable management of coastal aquifers is essential in Egypt, due to the increasing gap between water demand and available resources. Incidental recharge implies the provision of alternative water supplies to feed the recharge system, such as desalination plants and water reuse (Abd-Elaty et al., 2021b). The relocation of rice cultivations opens the way to a new range of possibilities, with relevant implications to the management of water in the study area (Salem et al., 2018). In the particular case of our study area, increasing the percentage of surface area for rice cultivation in the northern area of the NDA while reducing it in the central part, would

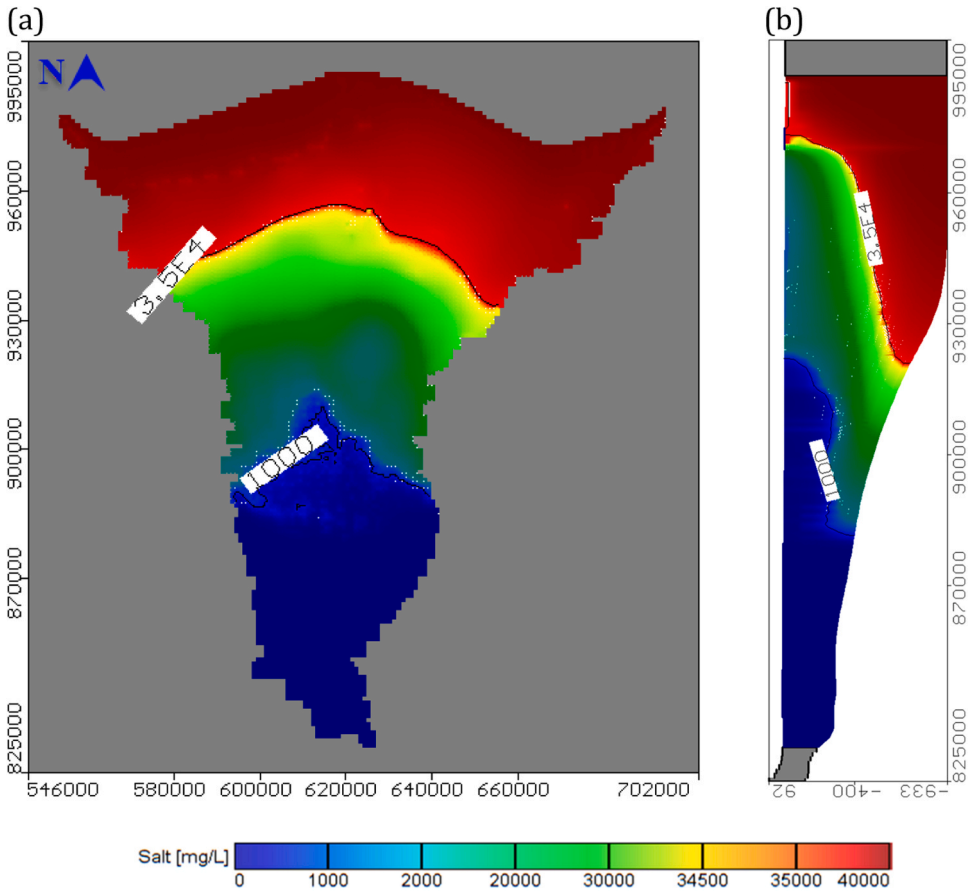

Fig. A3. Distribution of TDS for a SLR of 61 cm according to (a) aerial and (b) vertical longitudinal view.

certainly lead to short-term growth of costs in both economic and societal terms. However, this would happen at the benefit of much improved long-term sustainability, thanks to the inherent mitigation of the SWI.

The advantages of choosing the Nile Delta as a case study over others are primarily attributed to its unique regional characteristics. The relevance and representativeness of the Nile Delta make it an ideal area for conducting a focused analysis of water management and agricultural practices, considering its significant challenges related to SWI and SLR. Furthermore, the availability of comprehensive and reliable data sets, resulting from considerable research and data collection efforts in recent decades, enhances the precision and accuracy of analyses conducted in this region. While the Nile Delta offers valuable insights into SWI and SLR dynamics, it is worth noting that there are alternative case studies worldwide facing similar issues, such as the Gaza and the Biscayne aquifers. In such cases, the methodology presented in this work can be applied, taking into consideration the specific geographical conditions and selecting appropriate land use and crop rotation patterns.

4. Conclusions

This work investigates the effects of incidental recharge generated by the relocation of rice cultivation for contrasting SWI, in the NDA area. A three-dimensional SEAWAT numerical model was developed and tested under three different scenarios including (i) the impact of recharge location, (ii) sea level rise, and (iii) a combination of the two. The findings suggest that locating the rice cultivation in the northern part of the NDA effectively controled SWI, with Equi-line 35 showing substantial migration towards the coast. However, there are some model limitations to consider, including the quality and availability of the input data, such as hydrogeological parameters and recharge rates. Additionally, the model assumes certain simplifications and assumptions (i.e. steady-state conditions) which may not fully capture the dynamic nature of the NDA. Moreover, the model does not account for potential changes in land use and crop rotation patterns, which may influence recharge and SWI dynamics. To further improve the study, it is recommended to conduct field measurements and collect additional data to validate and refine the model. This would enhance the accuracy and reliability of the results. Incorporating climate change projections and assessing their influence on SWI dynamics and recharge patterns would enable a more robust evaluation of future scenarios.

In conclusion, the proposed modelling approach serves as a valuable tool for identifying optimal management strategies and predicting future scenarios in the NDA, especially in view of future climate-induced challenges, which may exacerbate the situation,

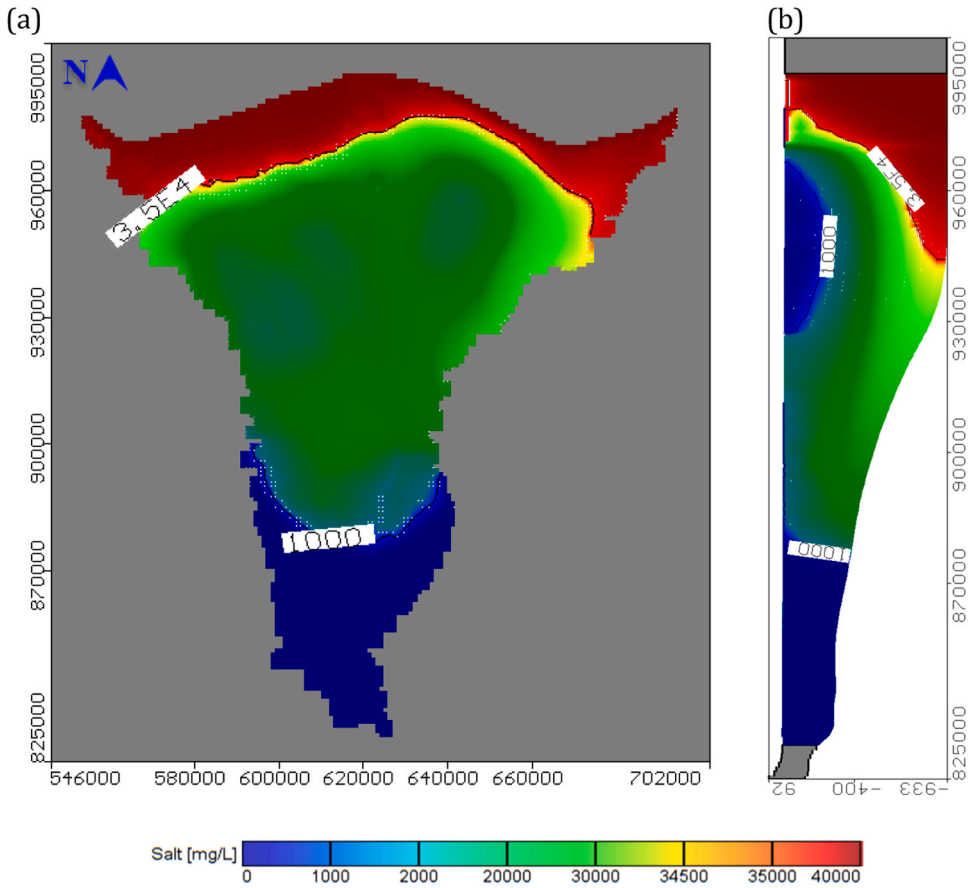

Fig. A4. Distribution of TDS for a SLR of 61 cm and recharge location at the north according to (a) aerial and (b) vertical longitudinal view.

requiring a proactive planning approach. The implementation of these strategies must be accompanied by a comprehensive evaluation of all the governance issues (economic, societal, environmental, etc.) in order to get the needed political consensus and finalise a well-coordinated implementation.

CRediT authorship contribution statement

Ismail Abd-Elaty, Gehan A. H. Sallam, Lorenzo Pugliese, Abdelazim M. Negm: Conceptualization, Methodology, Investigation, Formal analysis, Data curation. **Ismail Ismail Abd-Elaty, Gehan A. H. Sallam, Lorenzo Pugliese, Abdelazim M. Negm, Salvatore Straface, Ashraf Ahmed and Andrea Scozzari:** Visualization, Writing – original draft, Writing – review & editing, Resources. **Salvatore Straface, Ashraf Ahmed and Andrea Scozzari:** Supervision.

Declaration of Competing Interest

The authors declare that they have no known competing financial interests or personal relationships that could have appeared to influence the work reported in this paper.

Data Availability

No data was used for the research described in the article.

Acknowledgment

The authors are thankful to the Department of Water and Water Structures Engineering, Faculty of Engineering, Zagazig University, Zagazig 44519, Egypt, for constant support during the study.

Code availability

Upon request.

Appendix

See Appendix Fig. A1, Fig. A2, Fig. A3 and Fig. A4.

Appendix A. Supporting information

Supplementary data associated with this article can be found in the online version at doi:10.1016/j.ejrh.2023.101466.

References

Abd-Elaty, I., Polemio, M., 2023. Saltwater intrusion management at different coastal aquifers bed slopes considering sea level rise and reduction in fresh groundwater storage. Stoch. Environ. Res. Risk Assess.

Abd-Elaty, I., Zelenakova, M., 2022b. Saltwater intrusion management in shallow and deep coastal aquifers for high aridity regions. J. Hydrol. Reg. Stud. 40 https://doi.org/10.1016/j.ejrh.2022.101026.

Abd-Elaty, I., Sallam, G., Straface, A., Scozzari A, S., 2019a. Effects of climate change on the design of subsurface drainage systems in coastal aquifers in arid/semi-arid regions: case study of the Nile delta. Sci. Total Environ. J. 672, 283–295. https://doi.org/10.1016/j.scitotenv.2019.03.483.

Abd-Elaty, I., Abd-Elhamid, H.F., Nezhad, M.M., 2019a. Numerical analysis of physical barriers systems efficiency in controlling saltwater intrusion in coastal aquifers. Environ. Sci. Pollut. Res. 26 (35), 35882–35899. https://doi.org/10.1007/s11356-019-06725-3.

Abd-Elaty, I., Abd-Elhamid, H.F., Qahman, K., 2020. Coastal aquifer protection from saltwater intrusion using abstraction of brackish water and recharge of treated wastewater: case study of the Gaza aquifer. J. Hydrol. Eng. 25 (7), 05020012.

Abd-Elaty, I., Straface, S., Kuriqi, A., 2021a. Sustainable saltwater intrusion management in coastal aquifers under climatic changes for humid and hyper-arid regions. Ecol. Eng. 171, 106382 https://doi.org/10.1016/j.ecoleng.2021.106382.

Abd-Elaty, I., Shahawy, A.E.L., Santoro, S., Curcio, E., Straface, S., 2021b. Effects of groundwater abstraction and desalination brine deep injection on a coastal aquifer. Sci. Total Environ., 148928 https://doi.org/10.1016/j.scitotenv.2021.148928 (ISSN 0048-9697).

Abd-Elaty, I., Saleh, O.K., Ghanayem, H.M., Grischek, T., Zelenakova, M., 2021c. Assessment of hydrological, geohydraulic and operational conditions at a riverbank filtration site at Embaba, Cairo using flow and transport modeling. J. Hydrol.: Reg. Stud. 37. https://doi.org/10.1016/j.ejrh.2021.100900.

Abd-Elaty, I., Kushwaha, N.L., Grismer, M.E., Elbeltagi, A., Kuriqi, A., 2022a. Cost-effective management measures for coastal aquifers affected by saltwater intrusion and climate change. Sci. Total Environ. 836, 155656 https://doi.org/10.1016/j.scitotenv.2022.155656.

Abd-Elhamid, H., Javadi, A., Abd-Elaty, I., Sherif, M., 2016. Simulation of seawater intrusion in the Nile Delta aquifer under the conditions of climate change. Hydrol. Res. 47 (6), 1198–1210.

Abd-Elhamid, H.F., Javadi, A.A., 2008. Mathematical models to control saltwater intrusion in coastal aquifers. Proceeding of GeoCongress, New Orleans, Louisiana, USA.

Abdoulhalik, A., Ahmed, A.A., 2017a. The effectiveness of cutoff walls to control saltwater intrusion in multi-layered coastal aquifers: experimental and numerical study. J. Environ. Manag. 199, 62–73. https://doi.org/10.1016/j.jenvman.2017.05.040.

Abdoulhalik, A., Ahmed, A.A., 2017b. How does layered heterogeneity affect the ability of subsurface dams to clean up coastal aquifers contaminated with seawater intrusion. J. Hydrol. 553 (September), 708–721. https://doi.org/10.1016/j.jhydrol.2017.08.044.

Abdoulhalik, A., Abdelgawad, A.M., Ahmed, A.A., Moutari, S., Hamill, G., 2022. Assessing the protective effect of cutoff walls on groundwater pumping against saltwater upconing in coastal aquifers. J. Environ. Manag. 323, 116200.

Anwar, H.O., 1983. The effect of a subsurface barrier on the conservation of freshwater in coastal aquifers. Water Res. 17 (10), 1257–1265.

Bear, J., Cheng, A.H., Sorek, S., Quazar, D., Herrera, I., 1999. Seawater Intrusion in Coastal Aquifers, Concepts, Methods and Practices. Kluwer Academic publisher, Dordrecht, Netherlands (ISBN 0-7923-5573).

Costall, A.R., Harris, B.D., Teo, B., Schaa, R., Wagner, F.M., Pigois, J.P., 2020. Groundwater throughflow and seawater intrusion in high quality coastal aquifers. Sci. Rep. 10, 9866. https://doi.org/10.1038/s41598-020-66516-6.

Dasgupta, S., Hossain, M.M., Huq, M., Wheeler, D., 2018. Climate change, salinization and high-yield rice production in coastal Bangladesh. Agric. Resour. Econ. Rev. 47 (1), 66–89.

Diab, M.S., Dahab, K., El Fakharany, M., 1997. Impacts of the paleohydrological conditions on the groundwater quality in the Northern Part of Nile Delta, the Geological Society of Egypt. Geol. J. 4112B, 779–795 (Cairo).

El-Quilish, M., El-Ashquer, M., Dawod, G., Fiky, G.E., 2023. Development of an inundation model for the Northern Coastal Zone of the Nile Delta Region, Egypt using high-resolution DEM. Arab. J. Sci. Eng. 48 (1), 601–614.

ESA SL-CCI, 2018. ⟨http://www.esa-sealevel-cci.org/node/248⟩, (Accessed 3 December 2019).

Foster, S., Pulido-Bosch, A., Vallejos, A., Molina, L., Llop, A., MacDonald, A., 2018. Impact of irrigated agriculture on groundwater-recharge salinity: a major sustainability concern in semi-arid regions. Hydrogeology 26, 2781–2791.

Foster, S.S.D., Perry, C.P., 2009. Improving groundwater resource accounting in irrigated areas: a pre-requisite for promoting sustainable use. Hydrogeol. J. 18, 291–294.

Guo, W.X., Langevin Christian, D., 2002. User's Guide to SEAWAT: A Computer Program for Simulation of Three-Dimensional Variable-Density Groundwater Flow. USGS Techniques of Water Resources Investigations Book 6 Chapter A7, USA.

Hamza, M.S., Aly, A.I., Nada, A.A., Awad, M.A., 1988. Estimation of seepage from Ismailia Canal using Iodine 13. Isot. Prax. 24, 110–114.

Hunt, B., 1985. Some analytical solutions for seawater intrusion control with recharge wells. J. Hydrol. 80 (1–2), 9–18. https://doi.org/10.1016/0022-1694(85)90072-1.

Hussain, M.S., Abd-Elhamid, H.F., Javadi, A.A., Sherif, M.M., 2019. Management of seawater intrusion in coastal aquifers: a review. Water 11 (12), 2467.

Jasechko, S., Perrone, D., Seybold, H., Fan, Y., Kirchner, J.W., 2020. Groundwater level observations in 250,000 coastal US wells reveal scope of potential seawater intrusion. Nat. Commun. 11 (1), 3229.

Ketabchi, H., Mahmoodzadeh, D., Ataie-Ashtianib, B., Simmonsc, C., 2016. Sea-level rise impacts on seawater intrusion in coastal aquifers: review and integration. Hydrol. J. 535, 235–255. https://doi.org/10.1016/j.jhydrol.2016.01.083.

Klassen, J., Allen, D.M., 2017. Assessing the risk of saltwater intrusion in coastal aquifers. J. Hydrol. 551, 730–745.

Langevin, C.D., Guo, W., 2006. MODFLOW/MT3DMS-based simulation of variable-density groundwater flow and transport. Ground Water 44 (3), 339–351.

Langevin, C.D., Thorne, D.T., Jr., Dausman, A.M., Sukop, M.C., Guo, Weixing, 2008. SEAWAT Version 4: A Computer Program for Simulation of Multi-Spe.

Legeais, J.-F., Ablain, M., Zawadzki, L., Zuo, H., Johannessen, J.A., Scharffenberg, M.G., Fenoglio-Marc, L., Fernandes, M.J., Andersen, O.B., Rudenko, S., Cipollini, P., Quartly, G.D., Passaro, M., Cazenave, A., Benveniste, J., 2018. An improved and homogeneous altimeter sea level record from the ESA Climate Change Initiative. Earth Syst. Sci. Data 10, 281–301. https://doi.org/10.5194/essd-10-281-2018.

Lin, K., Lu, P., Xu, C.Y., Yu, X., Lan, T., Chen, X., 2019. Modeling saltwater intrusion using an integrated Bayesian model averaging method in the Pearl River Delta. J. Hydroinform. 21 (6), 1147–1162.

Luyun, R., Momii, K., Nakagawa, K., 2011. Effects of recharge wells and flow barriers on seawater intrusion. Ground Water 49, 239–249. https://doi.org/10.1111/j.1745-6584.2010.00719.x.

Meyer, R., Engesgaard, P., Sonnenborg, T.O., 2019. Origin and dynamics of saltwater intrusion in a regional aquifer: combining 3-D saltwater modeling with geophysical and geochemical data. Water Resour. Res. 55, 1792–1813. https://doi.org/10.1029/2018WR023624.

Molle, F., Gaafar, I., El-Agha D.E., Rap, E., 2016. Irrigation efficiency and the Nile Delta water balance. Water and Salt Management in the Nile Delta Project Report No. 9. IWMI, WMRI, Cairo, 2016.

Morsy, W.S., 2009. Environmental Management to Groundwater Resources for Nile Delta Region (PhD thesis). Faculty of Engineering, Cairo University, Egypt.

Motallebian, M., Ahmadi, H., Raoof, A., Cartwright, N., 2019. An alternative approach to control saltwater intrusion in coastal aquifers using a freshwater surface recharge canal. J. Contam. Hydrol. 222, 56–64.

MWRI, 2013. Proposed Climate Change Adaptation Strategy for the Ministry of Water Resources and Irrigation in Egypt (Tech. Report). Ministry of Water Resources and Irrigation, Egypt.

Negm, A.M., Sakr, S., Abd-Elaty, I., Abd-Elhamid, H.F., 2018. An overview of groundwater resources in Nile Delta Aquifer. In: Negm, A. (Ed.), Groundwater in the Nile Delta. The Handbook of Environmental Chemistry, 73. Springer, Cham. https://doi.org/10.1007/698_2017_193.

Nerem, R.S., Beckley, B.D., Fasullo, J.T., Hamlington, B.D., Masters, D., Mitchum, G.T., 2018. Climate-change–driven accelerated sea-level rise detected in the altimeter era. Proc. Natl. Acad. Sci., 201717312 https://doi.org/10.1073/pnas.1717312115.

Nossair, A.M., 2011. Climate Changes and Their Impacts on Groundwater Occurrence in the Northern Part of East Nile delta (MSc thesis). Faculty of Science, Zagazig University, Egypt.

Oude Essink, G.H., 2001. Salt water intrusion in a three-dimensional groundwater system in The Netherlands: a numerical study. Transp. Porous Media 43, 137–158. https://doi.org/10.1023/A:1010625913251.

Rasmussen, P., Sonnenborg, T.O., Goncear, G., Hinsby, K., 2013. Assessing impacts of climate change, sea level rise, and drainage canals on saltwater intrusion to coastal aquifer. Hydrol. Earth Syst. Sci. 17 (421–443), 2013. https://doi.org/10.5194/hess-17-421-2013.

RIGW, 1992. Groundwater Resources and Projection of Groundwater Development, Water Security Project. (WSP), Research Inst. for Groundwater, Kanater El-Khairia, Egypt, 1992b.

Roger, L.J., Kazuro, M., Kei, N., 2010. Effects of artificial recharge and flow barrier on seawater intrusion. Ground Water 49 (2), 239–249.

Roger, L.J., Kazuro, M., Kei, N., 2011. Effects of recharge wells and flow barriers on seawater intrusion. Groundwater 49, 239–249.

Roy, D.K., Datta, B., 2017. Genetic algorithm tuned fuzzy inference system to evolve optimal groundwater extraction strategies to control saltwater intrusion in multi-layered coastal aquifers under parameter uncertainty. Model. Earth Syst. Environ. 3, 1707–1725. https://doi.org/10.1007/s40808-017-0398-5.

Salem, Z.E., Gaame, O.M., Hassan, T.M., 2018. Integrated subsurface thermal regime and hydrogeochemical data to delineate the groundwater flow system and seawater intrusion in the middle Nile Delta, Egypt. In: Groundwater in the Nile Delta. Springer, Cham, pp. 461–486.

Shi, W., Lu, C., Werner, A.D., 2020. Assessment of the impact of sea-level rise on seawater intrusion in sloping confined coastal aquifers. J. Hydrol. 586, 124872.

SNC, 2010. Egypt's Second National Communication, Egyptian Environmental Affairs Agency (EEAA-May 2010). Under the United Nations Framework Convention on Climate Change on Climate Change.

Stocker, T.F., Qin, D., Plattner, G.-K., Tignor, M., Allen, S.K., Boschung, J., Nauels, A., Xia, Y., Bex, V., Midgley, P.M. (Eds.), 2013. Climate Change 2013: The Physical Science Basis. Contribution of Working Group I to the Fifth Assessment Report of the Intergovernmental Panel on Climate Change. IPCC, Cambridge, United Kingdom and New York, NY, USA, p. 1535 pp.

Tao, H., Al-Bedyry, N.K., Khedher, K.M., Shahid, S., Yaseen, Z.M., 2021. River water level prediction in coastal catchment using hybridized relevance vector machine model with improved grasshopper optimization. J. Hydrol. 598, 126477.

Tsanis, I.K., Song, L.F., 2001. Remediation of sea water intrusion: a case study. Groundw. Monit. Remediat. 21 (3), 152–161.

WMRI-NWRC, 2002. Unpublished Report under the Matching Supply and Demand Project, Water Management. Research Institute, National Water Research Center, Ministry of Water Resources and Irrigation, Egypt.

Xu, Z., Hu, B.X., Ye, M., 2018. Numerical modeling and sensitivity analysis of seawater intrusion in a dual-permeability coastal karst aquifer with conduit networks. Hydrol. Earth Syst. Sci. 22, 221–239. https://doi.org/10.5194/hess-22-221-2018.

Yossif, T.M., 2019. Land cover change monitoring in Egypt using satellite imagery. Int. J. Environ. 8, 151–161.